GL04030 JOURNAL OF GEOPHYSICAL RESEARCH, VOL. 86, NO. B12, PAGES 11,735–11,746, DECEMBER 10, 1981

Thermal Regime of the Escalante Desert, Utah, With an Analysis of the Newcastle Geothermal System

DAVID S. CHAPMAN, MONICA D. CLEMENT, AND CHARLES W. MASE[1]

Department of Geology and Geophysics, University of Utah, Salt Lake City, Utah 84112

Twenty-five new heat flow measurements are presented for the Escalante Desert region within the Great Basin of the western United States. Heat flow, excluding geothermal areas, ranges from 43 to 350 mW m^{-2}, but much of the variability may be caused by deeply circulating groundwater redistributing the regional flux. A subset of 10 sites drilled specifically to characterize the heat flow of the region yielded a mean of 100 mW m^{-2} with a standard deviation of 22 mW m^{-2}. A comparison of thermal conductivities of solid cylindrical discs and rock chips (rhyolite to andesite tuffs) confirmed the importance of porosity corrections to thermal conductivity measurements. A 'blind' geothermal system southwest of Newcastle, Utah, situated within the Escalante Desert, has also been studied. Temperatures of 110°C are observed only 75 m below the ground surface. Heat flow results from 11 drillholes in this region yield values between 163 and 3065 mW m^{-2}. The 500 mW m^{-2} contour encloses an area of 9.4 km^2. By integrating the excess heat flux (above background) over the thermal anomaly, we deduce a thermal power loss of 12.8 MW for this geothermal system, which corresponds to a subsurface water discharge of 32 kg s^{-1}.

INTRODUCTION

The Escalante Desert, Utah, is an elliptical (70 × 45 km) valley situated within the southeastern Great Basin about 50 km west of the Basin and Range–Colorado Plateau physiographic boundary (Figure 1). The valley is surrounded and underlain by Tertiary ash flow tuff sequences erupted between 29 and 12 m.y. before present. These tuffs represent one phase of widespread Cenozoic volcanic activity, which resulted in a belt of volcanic rocks covering southwestern Utah and extending west-northwest into Nevada (Figure 1).

Within this volcanic belt on the periphery of the Great Basin are found many of the known geothermal resource areas (KGRA) of the state of Utah: Roosevelt Hot Springs KGRA, Monroe-Red Hill Hot Springs KGRA, Joseph Hot Springs, Cove Fort-Sulphurdale KGRA, Thermo-Lund KGRA, and Newcastle KGRA (Figure 1). These geothermal systems derive their heat in a general sense from an additional crustal heat input associated with lithospheric extension and deep intrusions [see *Lachenbruch and Sass*, 1978; *Blackwell*, 1978, for discussion]. The systems may be locally driven either by heat from cooling silicic bodies within the crust, as is likely the case at Roosevelt Hot Springs [*Ward et al.*, 1978; *Wilson and Chapman*, 1981], or by forced convection of groundwater in a high geothermal gradient environment, as has been suggested for the Monroe-Red Hill system [*Kilty et al.*, 1979]. Important elements in understanding and characterizing these geothermal systems are the regional heat flow pattern surrounding and the thermal power loss within individual systems. The object of this paper is to document these elements for the Escalante Desert region of southwestern Utah. New heat flow values are presented which define the magnitude of the regional heat flow, and these data are in turn used for a more detailed analysis of the Newcastle geothermal system.

GEOLOGICAL SETTING

The geology of the Escalante Desert region is dominated by sequences of thin ash flow tuff sheets of rhyolitic to andesitic composition [*Rowley et al.*, 1978; *Hausel and Nash*, 1977], the stratigraphy of which is given in Figure 2. These rocks form the topographically high boundary ranges surrounding the Quaternary alluvial, colluvial, and lacustrine deposits of the valley floor [*Hintze*, 1963]. Sedimentary rocks of Paleozoic and Mesozoic age are found in the northeastern part of the Escalante Desert, and Cretaceous sediments (Iron Springs FM., Figure 2) crop out in the southeastern section in the Iron Springs district [*Hintze*, 1963; *Mackin*, 1947, 1960].These rocks were subjected to regional and local thrust faulting in the Sevier Orogeny and broad regional folding during the Laramide event [*Mackin*, 1947, 1960]. The early Tertiary Claron Formation (equivalent to the Wasatch Formation of the Colorado Plateau) was deposited on the nearly flat erosional surface of the pre-Cenozoic rocks [*Mackin*, 1960; *Rowley et al.*, 1978]. The earliest of the ash flow tuff units were deposited directly on the Claron Formation (Figure 2) and sometimes interfinger with it [*Mackin*, 1947]. Volcanic evolution along the entire belt (Figure 1) was episodic, with a major mid-Miocene hiatus in activity apparent, likely due to a complex response of this intraplate region to Farralon–Pacific–North American plate interactions on the west coast [*Noble*, 1972]. *Rowley et al.* [1978] have noted that the earliest volcanic sequences predate major episodes of Basin and Range rifting in this area. This suggests that Great Basin volcanism is not a simple response to lithospheric extension.

Intrusive rocks in the Escalante Desert region occur in an arcuate pattern on the southeastern border of the desert [*Mackin*, 1947, 1960; *Cook and Hardman*, 1967; *Rowley et al.*, 1978]. Although the intrusive outcrop is spatially restricted, the occurrence of a much larger body at depth is not precluded [*Mackin*, 1947, 1960; *Cook and Hardman*, 1967; *Schmoker*, 1972; *Pe*, 1980]. To date, however, there is no strong geological or geophysical evidence to support the hypothesis [*Crosby*, 1973] of a caldera origin for the valley [M. G. Best, personal communication; *Pe*, 1980].

Geophysical studies in the Escalante Desert have been restricted to regional gravity and magnetic surveys [*Cook and Hardman*, 1967; *Win Pe*, 1980], reconnaissance AMT surveys at the Lund and Newcastle KGRA's [*Gardner et al.*, 1976], and isolated heat flow determinations [*Wright*, 1966; *Costain and Wright*, 1973; *Rush*, 1977].

[1]Now with the U.S. Geological Survey, Menlo Park, California 94025.

Paper number 1B1334.
0148-0227/81/001B-1334$01.00

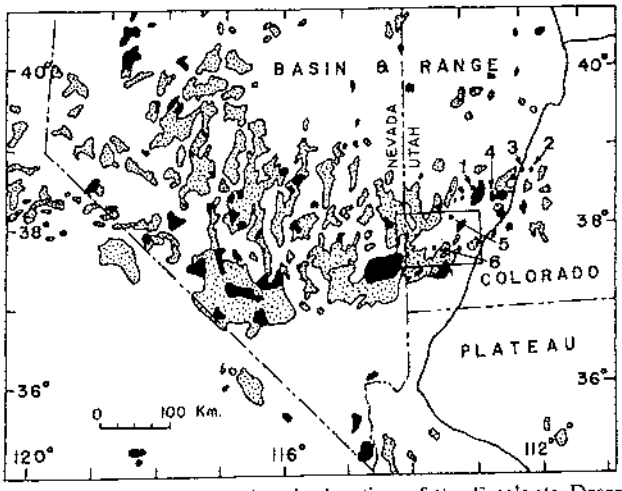

Fig. 1. Index map showing the location of the Escalante Desert (ED) in southwest Utah, and its proximity to the Basin and Range–Colorado Plateau physiographic boundary. Distribution of silicic igneous rocks younger than 34 m.y. old is also shown; dotted pattern represents silicic tuffs, solid pattern represents rhyolitic lava flows and intrusive rocks [after *Stewart and Carlson*, 1976]. Known geothermal resource areas (KGRA's) are marked as follows: 1, Roosevelt Hot Springs; 2, Monroe–Red Hill Hot Springs; 3, Joseph Hot Springs; 4, Cove Fort–Sulphurdale; 5, Thermo–Lund; 6, Newcastle.

HEAT FLOW OBSERVATIONS

Temperature Measurements

Temperatures in drillholes were measured with a thermistor probe connected by lightweight cable using three or four wire configurations to a Wheatstone Bridge or digital ohm meter, respectively, (details are similar to those described by *Roy et al.* [1968], *Sass et al.* [1971*b*] and Appendix I of *Chapman* [1976]). We used Fenwal K212E thermistor probes having a nominal resistance of 10,000 ohms at 20°C, power dissipation of 50 mW K^{-1} in still water, and response time of 5 s. The probes were calibrated with a platinum resistance thermometer by determining resistance R and temperature T pairs over the range 0–60°C and fitting them to a single curve of the form

$$R = \exp\left(A + \frac{B}{T + C}\right)$$

Residuals from these curves at calibration points did not exceed 0.03°C over the entire temperature range, indicating that more complicated curve fitting over limited segments of the temperature range [*Sass et al.*, 1971*b*] is not necessary for our purposes. For a thermistor temperature coefficient of −4% per degree typical of these probes, a ±1 ohm uncertainty in the resistance measurement at 20°C is equivalent to a temperature sensitivity of ±0.004 K. The accuracy of a field temperature measurement, however, is limited by accumulation of calibration errors and stability of the resistance meter and is closer to 0.1 K. Furthermore, the representativeness of any individual temperature measurement depends on the stability of the fluid filling the drillhole, not always known in detail. For this study, field measurements were made at discrete depth intervals, commonly 1–5 m, in drillholes after waiting at least one minute for the probe to equilibrate with its surroundings.

Temperature-depth profiles for 21 sites in and around the Escalante Desert (Figure 3) are shown in Figures 4–8. The drillholes vary in depth from 36 to 118 m, somewhat shallower than desired for purposes of regional heat flow determinations. Although more confidence is usually placed in results from deeper holes, the depth of drillhole alone is no guarantee of reliability; it is important to display the new temperature-depth data and to judge the reliability of a conductive heat flow assumption in the context of the data and the local geological conditions surrounding the site. For this region we will discuss separately five subsets of our new data. More complete details of each site, including location and elevation, borehole drilling and logging history, temperature-depth table, and lithology, can be found in Table 1, and appendix A of *Clement* [1980].

Temperature-depth profiles shown in Figure 4 are from 10 boreholes drilled in the ash flow tuffs around the periphery of the Escalante Desert (see Figure 3) specifically for heat flow

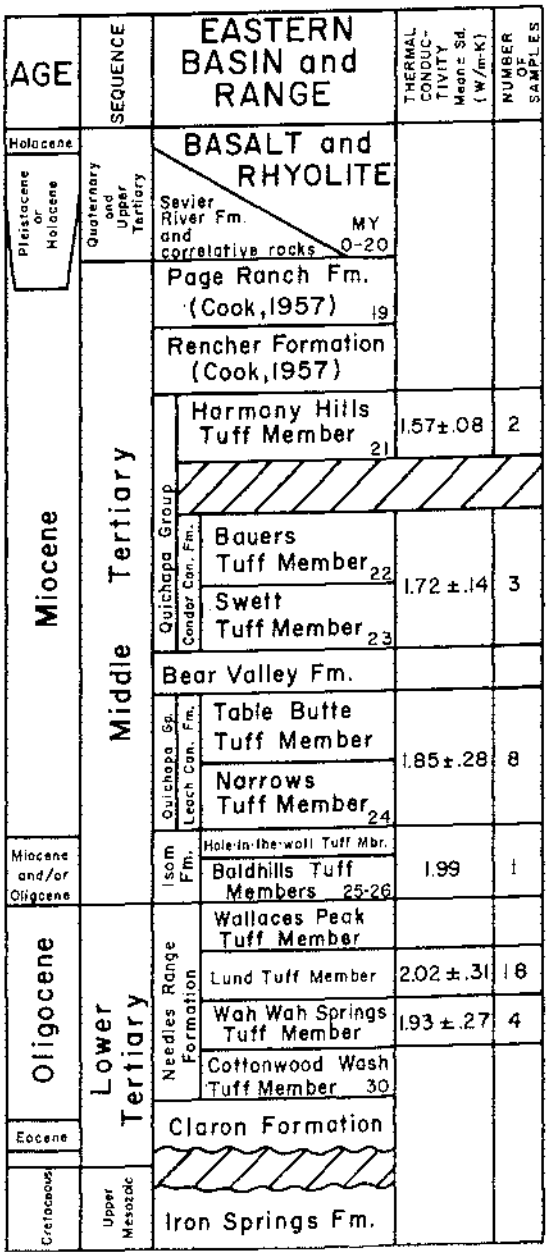

Fig. 2. Volcanic stratigraphy of the Escalante Desert region, southwest Utah [modified from *Rowley et al.*, 1978]. Thermal conductivity values of rock units are given and will be discussed later in the text.

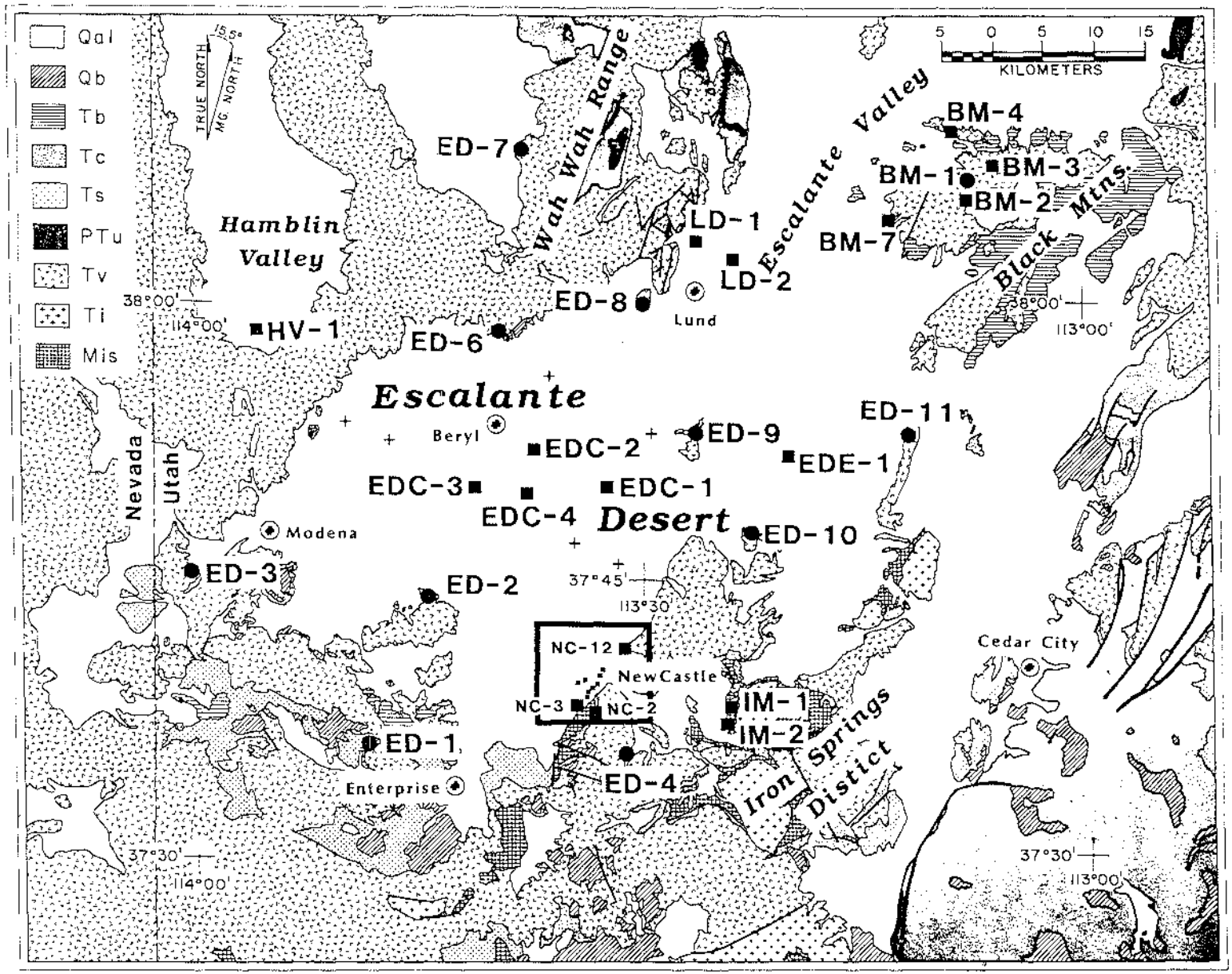

Fig. 3. Geologic map of Escalante Desert region southwest Utah [after *Hintze*, 1963], showing location of regional heat flow sites. Site designations match those in Table 1. The rectangular area near 37°40'N, 113°30'E encompasses the Newcastle geothermal system, discussed separately in the text. Geologic key: Qal, Quaternary alluvium and colluvium; Qb, Quaternary basalt; Tb, Tertiary basalt; Tc, Tertiary Claron formation; Tsu, undifferentiated Tertiary sediments; PTU, undifferentiated pre-Tertiary rocks; Tv, Tertiary silicic volcanics; Ti, Tertiary intrusives; Mis, Mesozoic Iron Springs Fm.

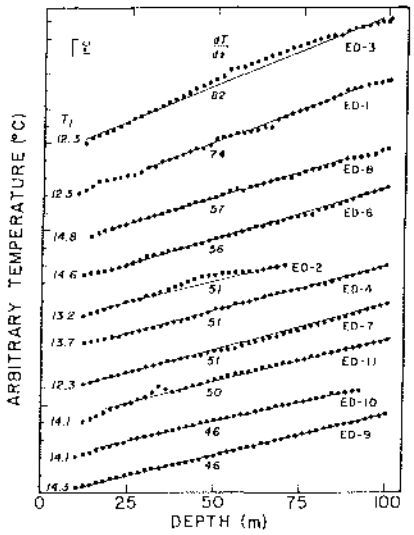

Fig. 4. Temperature-depth profiles for the ED series sites in tuffs surrounding the Escalante Desert (see Figure 3 for site locations). An arbitrary temperature scale is used to avoid overlap, but inclusion of the actual temperature T_1 of the shallowest point plotted permits the reconstruction of actual temperature profiles. Thermal gradient values given for the straight line segments marked.

determinations. Profiles from ED 9, 10, 7, 4, 6, and 8 yield consistent gradients characteristic of regions with conductive heat flux. ED 11 exhibits a disturbance at 35 m, as does ED 2 between 35 and 60 m and ED 1, intermittently, throughout the entire hole. In ED 2, 35–60 m was a zone of lost circulation; in ED 1, numerous fractures with flowing water were encountered throughout the hole. We believe that these temperature disturbances arise from minor groundwater flow in fractures or in the formation, but again the overall profiles are indicative of a predominant conductive flux. ED 3 has a gradient break at 50 m not entirely explicable by thermal conductivity contrasts, and it too may indicate minor groundwater flow. The thermal gradients attached to these data are indicated in Figure 3 by solid lines and are listed in Table 1. The average gradient from the 10 drillholes is 56.4°C km^{-1} and will henceforth be referred to as the 'background' gradient for the tuffs surrounding the Escalante Desert.

Another set of temperature-depth profiles found in sites on the northern margin of the Escalante Desert is shown in Figure 5. Sites HV 1, LD 1, and LD 2 all exhibit conductive behavior on the scale of the borehole, although the high gradient of 132°C km^{-1} in LD 1 and the contrast with results in LD 2 suggests to us a convective heat transfer enhancement at a deeper

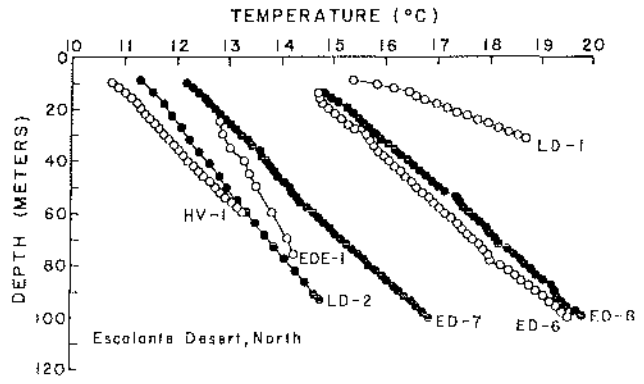

Fig. 5. Temperature-depth profiles for sites on the northern margin of the Escalante Desert (see Figure 3 for site locations).

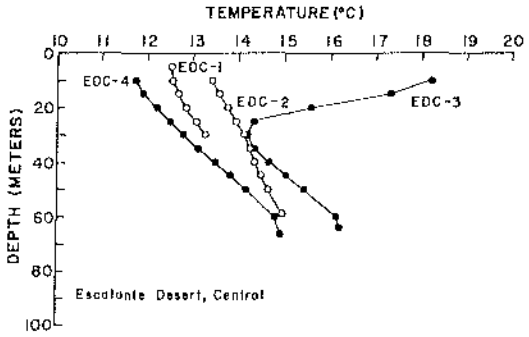

Fig. 6. Temperature-depth profiles for water wells within the central Escalante Desert (see Figure 3 for site locations).

level. Profiles at sites ED 6, 7, and 8 are repeated from Figure 4 for comparison purposes.

In contrast to the consistent and regular gradients in the ED series holes, measurements made in five shallow water wells in the central Escalante Desert (Figures 5 and 6) show greater irregularities and much less consistency between adjacent holes. EDC 3 and EDC 4 (Figure 6) are water wells adjacent to two deep geothermal test wells. *Goode* [1978] reports 149°C water produced from 2.1 km depth in the westernmost test well near EDC 3. Assuming a 12°C surface intercept temperature, a minimum gradient of 64°C km^{-1} is obtained for the geothermal test well. Gradients calculated for EDC 3 and EDC 4 are 68 and 66°C km^{-1}, respectively. Because the gradients in these two wells are very similar to that in the 2.1-km-deep well, EDC 3 and EDC 4 are taken as the more representative gradients. EDC 1, EDC 2 (Figure 6), and EDE 1 (Figure 5) also have consistent gradients of 41, 31, and 30°C km^{-1}, respectively, but they differ significantly from EDC 3 and 4 and the deep test well. These differences over lateral distances of a few kilometers are not uncommon among sites in Basin and Range alluvial valleys and suggest that all shallow gradients should be regarded with suspicion until checked against other and preferably deeper results.

Two profiles from boreholes separated by 1.3 km in the Iron Springs District vicinity are shown in Figure 7. While both profiles exhibit some irregularities, the consistent gradients of 24 and 28°C km^{-1} and similar extrapolated surface intercept temperatures lend weight to their reliability. Heat flow values determined for these holes are also consistent, with values pulished previously in the same district [*Sass and Munroe*, 1974].

A final example of local thermal regimes can be made of a composite temperature-depth plot (Figure 8) of sites located within a 144 km^2 area in the Black Mountains in the northeast Escalante Desert (see Figure 3). Average site separation is 4 km. Thermal gradients vary from 49°C km^{-1} in BM 1 to 178°C km^{-1} in BM 3. None of these holes exhibits strong irregularities which are symptomatic of convective heat transport on the scale of the borehole depth, yet the contrasting gradients in similar rock types imply heat flow sources within the upper crust. Unless a case can be made for sufficiently recent upper crustal intrusions (i.e., in the last 500, 000 years) which are still losing heat, the most plausible explanation for such gradient contrasts is a redistribution of heat flow patterns caused by deeply circulating groundwater moving over scales of several kilometers. These flow patterns can be revealed by heat flow surveys, but conclusive identification will not be possible until the spatial density of measurements is equiva-

lent to several sites per flow scale length and not several flow scale lengths per measurement, as is now most often the case.

Thermal Conductivity

All thermal conductivity values were determined using the modified divided bar designed by D. D. Blackwell (personal communication) and similar in operation to that described by *Roy et al.* [1968] and by *Sass et al.* [1971*b*]]. The bar was calibrated with standards of fused silica and crystalline quartz, using temperature dependent conductivity given by *Ratcliffe* [1959] and a procedure described by *Chapman* [1976], which accounts for lateral heat losses and sample contact resistance. Reproducibility of thermal conductivity determinations is typically better than 2%; interlaboratory agreement between measurements on identical samples has been shown to be about 3% [*Chapman*, 1976].

Thermal conductivities were determined for each site by measurement on drill core or chips, measurements on discs cut from hand samples, or by assigning values based on previous measurements (Table 1). In the case of the drillholes ED 1 through ED 11, between 11 and 16 composite drill chip samples from each hole were measured on the divided bar using the cell technique of *Sass et al.* [1971*a*]. Thermal conductivity values for the remaining sites were assigned on the basis of measurements made on samples of alluvium and on solid discs cored from hand samples of outcrops.

The solid discs of surface outcrop samples form the basis of a laboratory experiment designed to determine appropriate formation porosities and to demonstrate the importance of porosity corrections to the measured chip conductivities of these rhyolite to andesite tuffs. Thermal conductivity values determined for drill chips using the cell technique [*Sass et al.*, 1971*a*] corresponds to the conductivity k_s of the solid component only. To determine the formation or in situ conductivity k_r, the measured conductivity of the solid component must be combined with an estimate of formation or rock porosity ϕ_o. The simplest model generally used leads to the relationship

$$k_r = k_w^{\phi_o} k_s^{(1-\phi_o)}$$

where k_w is the conductivity of water. For an appropriate range of solid component conductivities encountered in this study, Figure 9 illustrates the effect that porosity has on formation conductivity and consequently on heat flow determinations. For example, although porosities determined by simple vacuum saturation methods reveal that 77% of the samples have a porosity of 10% or less (Figure 9, bottom), for a conductivity range of 1.5–3.5 W m^{-1} K^{-1}, even a 10% porosity adjusts the measured chip conductivity and, consequently, the resulting heat flow downward between 9 and 16%.

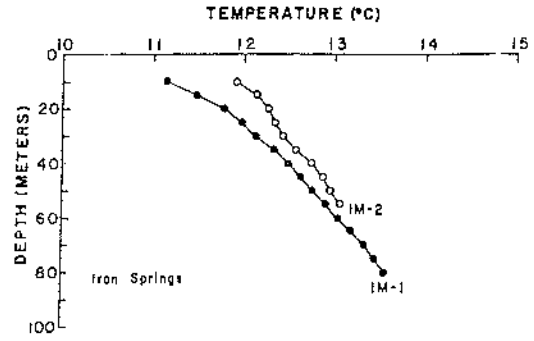

Fig. 7. Temperature-depth profiles for sites in the Iron Springs District (see Figure 3 for site locations).

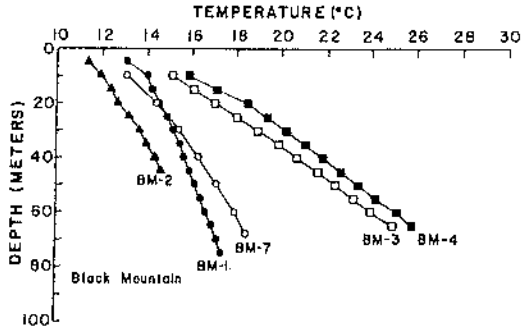

Fig. 8. Temperature-depth profiles for sites in the Black Mountain District (see Figure 3 for site locations).

Our porosity–thermal conductivity analysis involved drilling sixty-nine cylindrical cores from forty-one hand samples of outcrops near sites ED 2 through ED 11. Porosities were determined by weighing dry and vacuum saturated discs. After the saturated disc conductivities k_r were determined, the discs were crushed and the solid chip conductivities k_s were measured using the cell technique. Measured disc porosities ϕ_o were applied to determine a porosity corrected conductivity k_{pc}

$$k_{pc} = k_w^{\phi_d} k_s^{(1-\phi_d)}$$

for a comparison with the disc value. Details for each sample are given in appendix B of *Clement* [1980]; results of the test are shown in Figure 10. Whereas the uncorrected chip values (solid component k_s) fall systematically 10% or more above the disc values k_r, the porosity-corrected k_{pc} and disc conductivities agree much better (regression results: $k_{pc} = 1.06$, $k_r - 0.01$, correlation coefficient 0.93). It is interesting to note that the 6% deviation from a one to one correspondence is similar in magnitude and sense to that reported by *Sass et al.* [1971*a*] for their group V porous rocks, suggesting that this deviation may be systematic. The deviation could be caused by incomplete saturation of discs, which would have two effects: a measurement of k_r less than the true fully saturated k_r and an apparent lower porosity and hence underestimation of the porosity correction. Alternatively, the crushing and cell loading process may lead to a loss of a powder (low-conductivity clay) fraction and inadvertent enhancement of a resistive (high-conductivity quartz) fraction. A further possibility is that the aggregate chip-water mix in the cells is not adequately described by the mixing law chosen. In view of the uncertainty in downhole porosity and of inherent variability in rock conductivity, such deviations are quite tolerable. Hence all chip thermal conductivity values subsequently cited have been corrected for formation porosity, determined from laboratory measurements on representative hand and core samples.

Heat Flow, Escalante Desert

Heat flow values computed as the product of least squares temperature gradients over a specified depth interval and the harmonic mean thermal conductivity of samples from the same interval are given in Table 1 and shown in Figure 11 for 25 regional sites (excluding NC sites, Table 1) in and around the Escalante Desert. Site locations, elevations, depth intervals over which heat flow is computed, and the number and

TABLE 1. Basic Data for Escalante Desert Heat Flow Sites

Locality	Site	North Latitude	West Longitude	Elevation, m	Depth Range, m	Gradient, °C/km	N	k, W/m K	q, mW/m^2
				Regional Heat Flow Sites					
Escalante Desert	ED 1	37°36′23″	113°48′52″	1747 ± 5	30–92	74 ± 7	11	1.5 ± 0.1	111 ± 13 (87 ± 11)
	ED 2	37°44′20″	113°44′56″	1602 ± 2	12–70	51 ± 5	10	2.3 ± 0.1	115 ± 11
	ED 3	37°44′20″	114°02′19″	1750 ± 3	12–100	82 ± 4	16	1.8 ± 0.1	143 ± 10
	ED 4	37°36′53″	113°01′06″	1735 ± 3	20–100	51 ± 3	14	2.0 ± 0.1	102 ± 8 (83 ± 6)
	ED 6	37°59′05″	113°39′20″	1743 ± 3	22–100	56 ± 3	14	1.7 ± 0.1	97 ± 5
	ED 7	38°07′11″	113°37′41″	1862 ± 3	12–100	51 ± 2	16	2.4 ± 0.1	122 ± 7 (102 ± 5)
	ED 8	37°59′59″	113°31′13″	1643 ± 2	20–88	57 ± 3	11	2.2 ± 0.1	125 ± 9
	ED 9	37°53′00″	113°26′12″	1600 ± 2	12–100	46 ± 1	16	1.4 ± 0.1	67 ± 3
	ED 10	37°47′41″	113°22′43″	1655 ± 3	10–92	46 ± 2	15	1.9 ± 0.1	87 ± 6
	ED 11	37°52′51″	113°11′56″	1692 ± 3	12–100	50 ± 6	16	1.9 ± 0.1	93 ± 12
Escalante Desert, Central	EDC 1	37°50′20″	113°32′41″	1560 ± 1	20–30	41 ± 1	I	1.4 ± 0.2	58 ± 8
	EDC 2	37°52′28″	113°37′04″	1563 ± 1	10–59	31 ± 2	A	1.4 ± 0.2	43 ± 7
	EDC 3	37°50′20″	113°41′14″	1566 ± 1	35–64	68 ± 10	A	1.4 ± 0.2	96 ± 20
	EDC 4	37°50′08″	113°37′53″	1563 ± 1	20–60	66 ± 2	A	1.4 ± 0.2	92 ± 13
Escalante Desert, East	EDE 1	37°53′09″	113°19′56″	1585 ± 2	25–70	30 ± 4	A	1.4 ± 0.2	42 ± 9
Hamblin Valley	HV 1	37°59′05″	113°57′02″	2021 ± 3	16–60	49 ± 2	B	1.6 ± 0.2	78 ± 10
Lund	LD 1	38°03′29″	113°26′22″	1579 ± 2	11–31	132 ± 10	C	1.7 ± 0.2	224 ± 31
	LD 2	38°02′37″	113°24′03″	1548 ± 1	14–93	40 ± 1	B	1.6 ± 0.2	64 ± 8
Black Mountain	BM 1	38°06′43″	113°07′30″	1762 ± 3	25–75	49 ± 2	9	1.5 ± 0.1	74 ± 3
	BM 2	38°05′18″	113°08′12″	1865 ± 3	15–45	78 ± 8	E	1.5 ± 0.2	116 ± 17
	BM 3	38°07′26″	113°06′02″	1737 ± 3	10–65	178 ± 5	F	2.0 ± 0.1	350 ± 11
	BM 4	38°08′57″	113°08′34″	1612 ± 1	20–65	163 ± 5	G	1.6 ± 0.2	255 ± 33
	BM 7	38°04′40″	113°12′53″	1632 ± 2	20–68	84 ± 6	E	1.5 ± 0.2	125 ± 15
Iron Mountain	IM 1	37°38′12″	113°24′43″	1904 ± 3	35–80	28 ± 1	H	3.7 ± 0.4	101 ± 11
	IM 2	37°37′31″	113°24′30″	1912 ± 3	15–55	24 ± 3	H	3.7 ± 0.4	87 ± 13
				Newcastle Geothermal System Heat Flow Sites					
Newcastle	NC 2	37°38′05″	113°33′18″	1774 ± 12	46–89	89 ± 3	D	1.8 ± 0.2	163 ± 15
	NC 3	37°38′18″	113°34′06″	1643 ± 6	46–89	116 ± 4	D	1.8 ± 0.2	212 ± 20
	NC 4	37°38′26″	113°33′59″	1658 ± 6	8–91	199 ± 12	D	1.8 ± 0.1	349 ± 27
	NC 5	37°39′08″	113°33′34″	1631 ± 3	8–36	1869 ± 78	D	1.6 ± 0.1	3065 ± 275
	NC 6	37°38′56″	113°33′50″	1634 ± 3	5–38	1065 ± 102	D	1.6 ± 0.1	1747 ± 218
	NC 7	37°39′37″	113°33′03″	1619 ± 3	11–91	309 ± 24	D	1.8 ± 0.1	541 ± 49
	NC 8	37°39′51″	113°33′02″	1617 ± 3	17–41	1028 ± 30	D	1.8 ± 0.1	1871 ± 69
	NC 9	37°40′00″	113°32′52″	1618 ± 1	23–84	475 ± 58	D	1.8 ± 0.1	874 ± 116
	NC 10	37°39′34″	113°33′51″	1603 ± 2	0–40	1833 ± 100	D	1.6 ± 0.1	3006 ± 238
	NC 11	37°39′18″	113°34′15″	1600 ± 3	15–46	1292 ± 45	D	1.8 ± 0.1	2351 ± 97
	NC 12	37°41′21″	113°31′26″	1619 ± 3	49–118	21 ± 3	D	1.6 ± 0.2	35 ± 6

Thermal conductivity code: A = alluvium sample from EDC 1, 35% porosity ±10%; B = alluvium from EDC 1, 25% porosity ±10%; C = alluvium from EDC 1, 20% porosity ±10%; D is based on 8 downhole chip measurements from a well 100 feet NW of NC 10, porosity corrected ±10%; E is from BM 1 ±10%; F = mean ED 7, 8 hand sample data ±10%; G = mean ED 7, 8 hand sample, 20% porosity ±10%; H = mean Iron Springs Fm, *Sass and Munroe* [1974] ±10%; N is number of conductivity samples; heat flow values in parentheses are corrected for topography.

nature of conductivity samples is also given. Further details, including raw temperature-depth, conductivity-depth, and lithology-depth data, are given in appendix A of *Clement* [1980]. Topographic corrections to heat flow have been calculated following the technique of *Birch* [1950] and have been applied to sites where the correction is 5% or greater.

Heat flow at the twenty-five regional sites in Table 1 (excluding NC sites) ranges from 43 to 350 mW m^{-2} with a mean and standard deviation of 112 and 69 mW m^{-2}, respectively. It has long been held in heat flow studies that linearity in temperature-depth profiles is the principal criteria for evaluating whether heat is being transferred conductively or by convection. Those sites with reasonably linear temperature-depth behaviour or patterns that can be explained by the thermal conductivity structure are thought to be characterized by conductive flux and have traditionally been used to compute geotherms for the entire crust. However, results from several heat flow studies in the western U.S. cordillera (Table 2) now indicate that heat flow at these pseudoconductive sites has a higher degree of variability and changes more rapidly over short lateral distances than would be expected for an entirely conductive thermal regime. One obvious explanation for this variability is the deep circulation of groundwater to depths of kilometers and redistribution of part of the regional heat flux over distances of tens of kilometers. The unfortunate consequence of this realization for heat flow studies is the necessity either to be very selective in the geologic environment of heat flow sites so that deep groundwater effects can be avoided or to increase the spatial density of measurements to the point where the groundwater flow patterns are delineated and evaluated [*Kilty and Chapman*, 1980]. In many respects this situation is similar to the interpretation of oceanic heat flow results that evolved throughout the last decade.

We believe for several reasons that the simple mean heat

flow of 112 mW m^{-2} does not characterize the regional heat flux for the Escalante Desert: (1) results from EDC 1 and 2 are inconsistent with EDC 3 and 4 and more importantly inconsistent with a 1200-m-deep well only 8 km away, (2) the high heat flow at Black Mountains, in particular BM 3, cannot be sustained to great depths in the crust, and (3) the two Lund values differ by almost a factor of four, although they are obtained at sites only 4 km apart. However, simply eliminating inconsistent data lacks some objectivity. In the case of this study we do have a subset of sites which were drilled specifically for regional heat flow purposes in locations chosen so as to minimize topographic and hydrologic disturbances. These sites (ED 1–11, Table 1 and Figure 11) exhibit a narrower heat flow range and less scatter than the entire regional set. We take their mean heat flow of 100 mw m^{-2} (standard deviation 22 mW m^{-2}) to be representative of the Escalante Desert regional flux.

Heat flow in the east-central Escalante Desert is lower than normal, but is consistent with data taken in the vicinity of the Thermo Hot Springs in the Escalante Valley to the north [*Rush*, 1977]. Subnormal heat flow in the center of a basin has also been observed by *Sass and Sammel* [1976] in the Lower Klamath Lake Valley. Abnormally high heat flow is observed in the Black Mountains at sites BM 3 and 4. These sites may have some high temperature geothermal potential, although a more likely explanation for their enhanced heat flow is the existence of a warm water aquifer at a depth of a few hundred meters. Our new heat flow values in the Iron Springs District (Figure 11) are consistent with earlier measurements in the region [*Sass and Munroe*, 1974].

Heat Flow, Newcastle Geothermal System

The Newcastle region in the southeastern Escalante Desert (Figures 3, 11), is of interest because it can properly be called a 'blind" geothermal system. There are no surface hot springs or deposits here, and it was not until 1975, when boiling water (108°C) was encountered at about 70 m during the drilling of an irrigation well, that active geothermal interest was spurred.

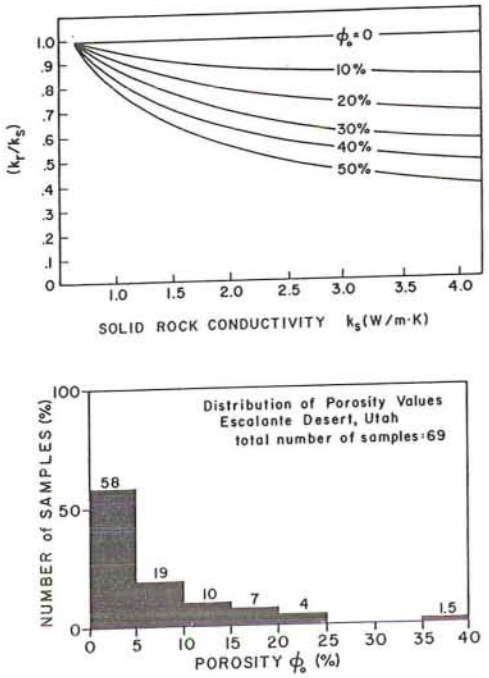

Fig. 9. (top) Relationship between thermal conductivity k_r of a porous rock saturated with water and the thermal conductivity k_s of the solid component for a range of rock porosities ϕ_0. Water conductivity used in the calculation is 0.6 W m^{-1} K^{-1} (bottom) Histogram of rock porosities for the Escalante Desert tuffs.

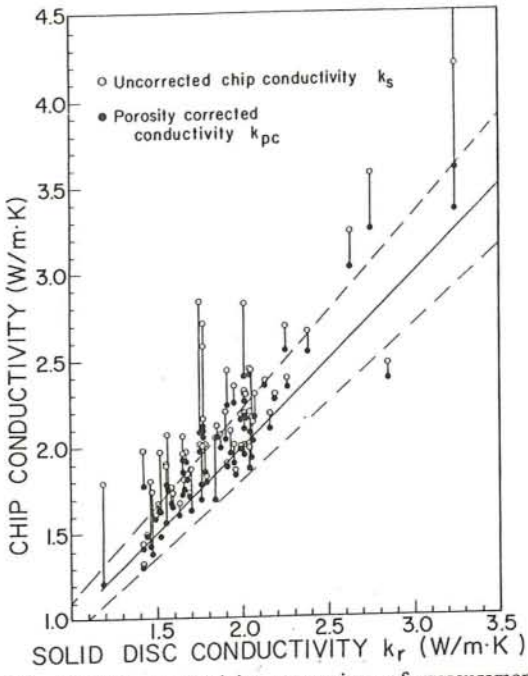

Fig. 10. Thermal conductivity comparison of measurements on rock discs and identical rock crushed into chips (*a*) uncorrected for rock porosity (open circles) and (*b*) corrected for rock porosity (closed circles). Solid line shows one to one correspondence; dashed lines show ±10% deviation.

Temperature-depth profiles for the Newcastle area shown in Figure 12 are based on data from *Rush* [1977]. The profiles exhibit many features such as subnormal gradients, downward curvature, isothermal sections, and temperature reversals that are now recognized to be characteristic of many geothermal systems [*Bodvarsson*, 1973; *Lachenbruch et al.*, 1976; *Sass and Sammel*, 1976; *Sorey et al.*, 1978; *Mase et al.*, 1979].

These features are caused by fluid motion in recharge, discharge, and lateral flux regions, respectively, where a substantial quantity of heat is being transferred by moving water. Only one site, NC 12, 3 km northeast of Newcastle (Figure 13) has a subnormal gradient (21°C km^{-1}) indicative of a hydrologic recharge zone. The remaining ten sites have elevated near surface gradients above 89°C km^{-1}. Whereas NC 2, 3, and 4 exhibit constant gradients, the temperature patterns at NC-6, 8, 9, and 11 become isothermal or reverse between 75 and 100 m, suggesting a thermal leakage aquifer at those depths. This depth range also corresponds to a 'coarse to pebbly' section (R. Stoker, written communication, 1980) and it is not unreasonable to postulate hot water moving laterally through this more permeable zone and losing heat conductively through the overlying material.

Thermal conductivity determinations were made on eight downhole composite drill chip samples obtained from a 152-m-deep well near NC 10. The entire section is alluvial; volcanic silts and sands with quartzite chips from the Iron Springs or Claron Formations (Figure 3) and varying degrees of carbonate cement. A mean value of 1.76 W m^{-1} K^{-1} was assigned for this material.

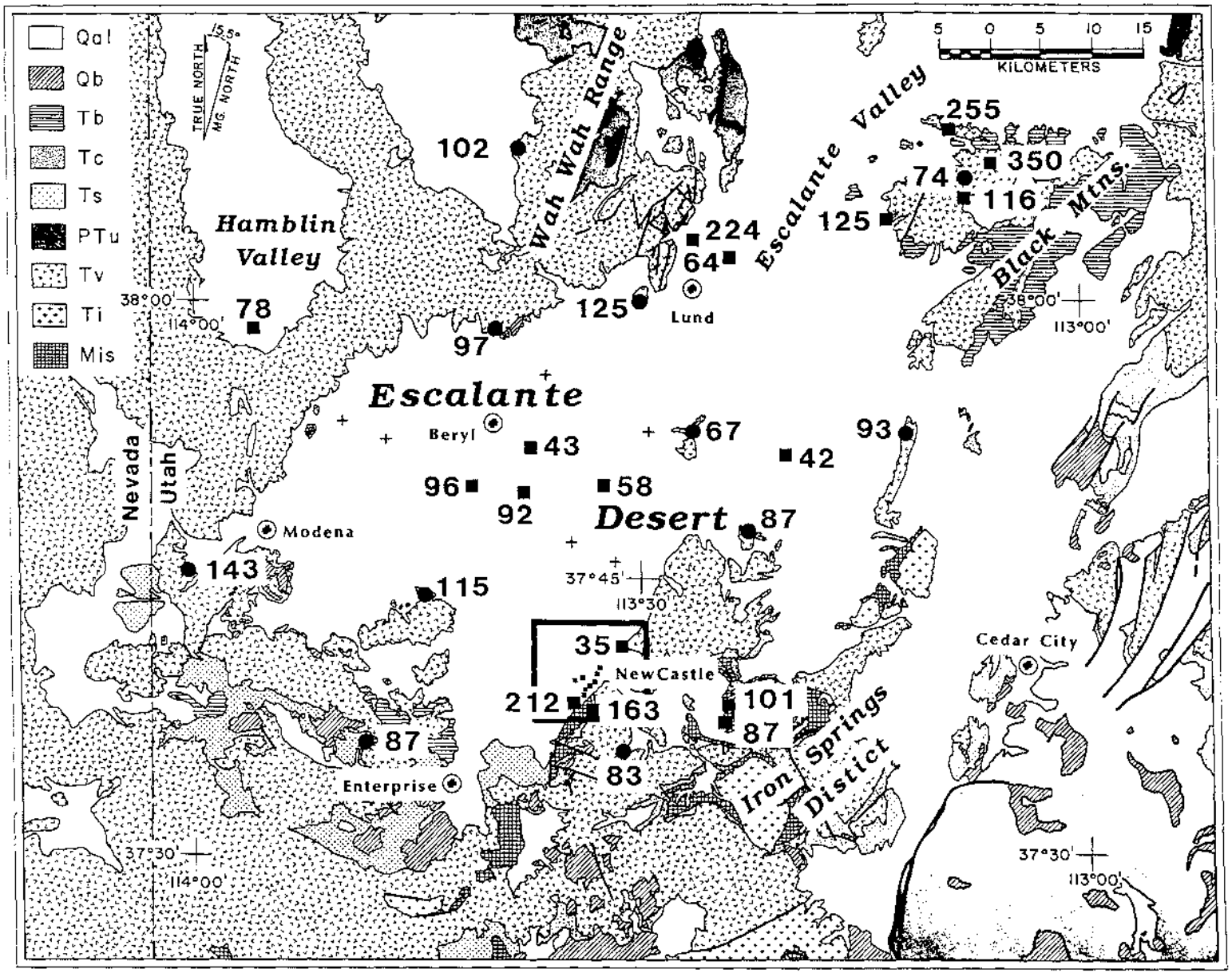

Fig. 11. Geologic map of Escalante Desert region (ibid. Figure 3) showing heat flow categories of heat flow sites and heat flow values in mW m^{-2}. Circles indicate sites where thermal conductivity samples from the drillhole were available; squares indicate sites where conductivity samples were collected from nearby outcrops or other drillholes. Heat flow values for the Newcastle geothermal system are show in Figure 13.

TABLE 2. Heat Flow Variations in Regions of the Western U.S. Cordillera Exclusive of Geothermal Zones

Region	N	Heat Flow, mW m^{-2} minimum	maximum	mean	s.d.	Source
Tucson	11	65	124	88	17	*Sass et al.* [1971*b*]
Southeast Oregon	15	46	96	65	14	*Sass et al.* [1976]
Klamath Falls	17	12	130	71	32	*Sass and Sammel* [1976]
Escalante Desert[a]	25	43	350	112	69	this paper
Escalante Desert[b]	10	67	125	100	22	this paper

Data restricted to sites which exhibit reasonably linear temperature-depth profiles. N is number of sites, s.d. is standard deviation.
[a] All data.
[b] Selected sites (see text).

Heat flow values for the 11 NC sites were computed using this average thermal conductivity and a geothermal gradient calculated for the upper section of each hole. Because of the magnitude of the gradients, the annual temperature wave is overwhelmed within 5 m of the surface, meaning that extremely shallow data may be used. Furthermore, the observations that most of the temperature-depth profiles have an upper linear section and extrapolate to about 15°C, the mean annual soil temperature for the Escalante Desert, support the assumption of a near surface conductive heat flux over this geothermal system, although deeper heat transfer is obviously convective. The resulting heat flow values in such a case will be of little regional significance but will be useful in determining the nature and magnitude of heat loss from the convective system.

Heat flow results for the Newcastle geothermal system are given in Table 1 and are shown as a contoured map in Figure 13. The thermal anomaly is constrained to the southwest by sites NC 2, 3, and 4 and to the northeast by site NC 9, but lack of heat flow sites to the north, northwest and southeast leave the anomaly unconstrained in those directions. Additional constraints are provided by estimating thermal gradients in irrigation wells under the assumption that observed water temperatures represent temperatures at the bottom of the well and converting those gradients to lower limit heat flow values. The resulting shape of the heat flow contours (Figure 13) considered together with the temperature-depth profiles (Figure 12) suggest a vertical upwelling zone which includes at least sites NC 5 and NC 10 and a broad lateral leakage zone to the north.

We now make an estimate of the heat loss for the Newcastle geothermal system by integrating the anomalous flux over the heat flow map shown in Figure 13. Details of the integration are given in Table 3. The anomalous heat loss within the 9.4 km^2 enclosed by the 500 mW m^{-2} contour above a background flux of 100 mW m^{-2} is about 13 MW. Other heat losses, namely in the region outside the 500 mW m^{-2} contour yet still above background, are unaccounted for. Also the temperature reversal at site NC 11 (see Figure 12) suggests that a cool region exists below the hot leakage zone and that this region may also absorb a fraction of the real heat loss. However, we have no data to constrain the magnitude of these latter effects and therefore will use the calculated value of 13 MW as a minimum for the system. The age of known volcanism in the region (29–12 m.y. before present) precludes the volcanics being related directly to a heat source for the geothermal system and suggests that the system is supported by circulating groundwater which is heated by a regional heat flow. The area over which some fraction of normal heat flow is extracted (i.e., if heat discharge is balanced by recharge in other parts of the system) in order to heat water circulating through the Newcastle system is substantial: all the flux over an area of 130 km^2, one third the background flux over an area of about 390 km^2 or an equivalent combination. It remains an important problem to substantiate this model of deep circulation and regional heating by mapping the subnormal heat flow area in such systems.

By knowing the thermal power loss of a system such as this, one can compute several related quantities. Assuming that the anomalous heat discharge rate is supported by mass flow, minimum mass discharge rates (m_D) and volume discharge rates (v_D) are given by

$$m_D = \frac{P}{c_f(T_R - T_0)} \qquad v_D = \frac{P}{\rho_f c_f(T_R - T_0)}$$

where P is the observed thermal power loss, c_f the specific heat of the fluid, ρ_f the density of the fluid, and T_r and T_0 the reservoir and surface temperatures respectively.

Using the following:

$$P = 12.8 \times 10^6 \text{ Watts}$$
$$c_f = 4.18 \times 10^3 \text{ J kg}^{-1} \text{ K}^{-1}$$
$$\rho_f = 10^3 \text{ kg m}^{-3}$$
$$T_r = 110°\text{C}$$
$$T_0 = 15°\text{C}$$

we calculate $m_D = 32$ kg s^{-1} and $v_D = 0.032$ m^3 s^{-1}. If the reservoir of lateral discharge below the thermal anomaly is considered to have an area of 9.4 km^2 (Table 3), to extend from

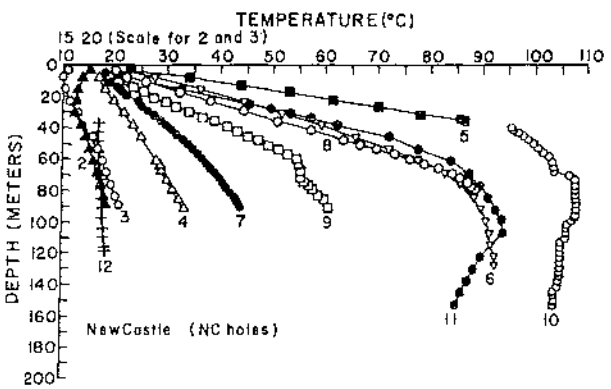

Fig. 12. Temperature-depth profiles for the Newcastle geothermal system. Numbers on profiles correspond to the NC site designation in Table 1. Location of sites is shown in Figure 13.

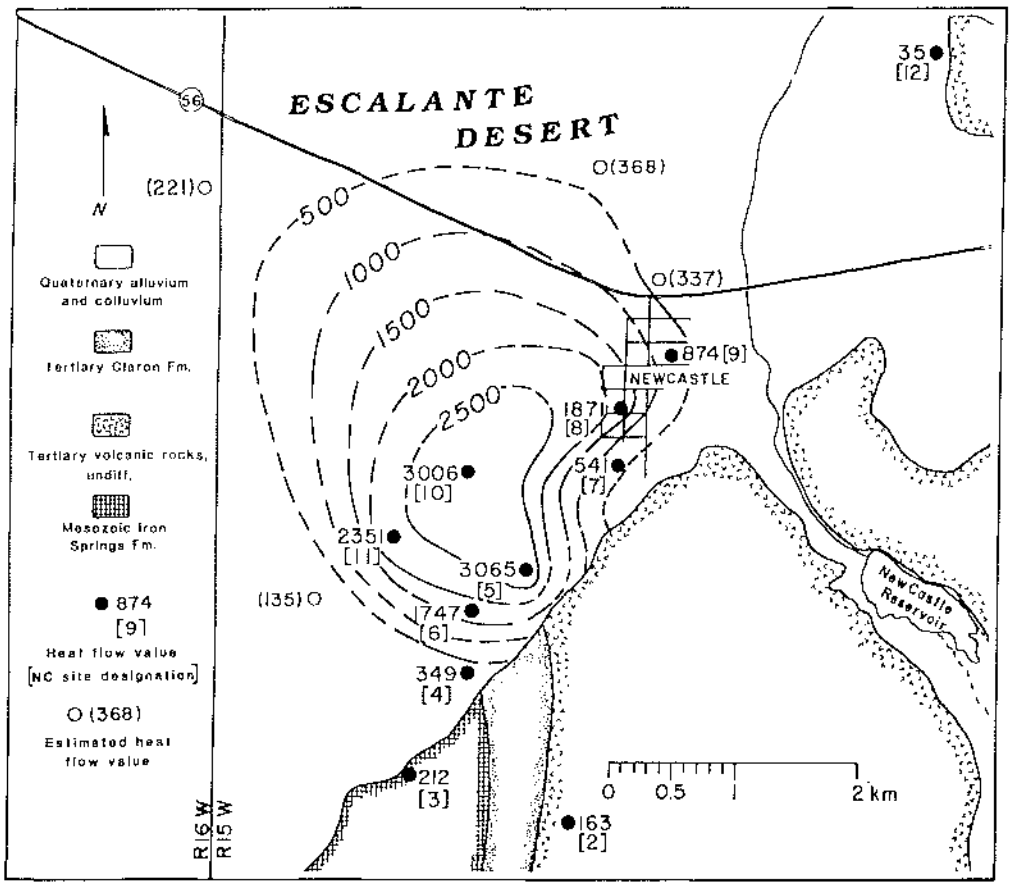

Fig. 13. Heat flow map for the Newcastle geothermal system. Heat flow values and contour values are given in mW m^{-2}. Solid circles indicate sites where heat flow is computed from actual temperature-depth aand conductivity measurements. Open circles represent estimates based on temperatures in irrigation wells. Heat loss from this system is compiled in Table 3.

75 to 100 m on the basis of temperature-depth profiles (Figure 12), and have a 15% porosity, the mass of water in the reservoir is 3.5×10^{10} kg. The replacement time for this water is 1.1×10^9 s or 35 years.

In terms of utilizing this geothermal system, the total useful heat will be that at depth in the upflow region. However, the minimum useful heat will be that measured in this study, about 13 MW thermal produced by 32 kg s^{-1} mass flow. Permeability factors will determine how much extra fluid can be economically extracted.

We may also evaluate the Newcastle geothermal system using the formalism of *Brook et al.* [1978], although some qualifications must be placed on the appropriateness of such an analysis for this type of a geothermal system. In particular, as opposed to low-permeability, high-temperature reservoirs where resupply of heat may be a small fraction of energy producible from storage alone, the Newcastle system may be in a quasi steady state condition whose life time is limited only by the natural sealing of the system, perhaps taking as long as 1 Ts (1 Terra second = 10,000 years). In spite of this it is still useful for comparison purposes to compute the reservoir thermal energy Q_R given by [*Brook et al.*, 1978, equation 1]

$$Q_R = (\rho c)\, AD\, (T_R - T_0)$$

where ρc is the volumetric specific heat of rock plus water, assuming a 15% reservoir porosity, A the reservoir area, D the reservoir thickness and T_R and T_0 the reservoir and surface temperatures, respectively. We use the following values:

$$\rho c = 2.7 \times 10^6 \text{ J m}^{-3} \text{ K}^{-1}$$

$$A = 9.4 \times 10^6 \text{ m}^2$$

(see Table 3)

$$D = 25 \text{ m}$$

$T_R = 110°C$ (see Figure 12)

$T_0 = 15°C$ (see Figure 12)

to obtain a value $Q_R = 6.0 \times 10^{16}$ J. The least certain parameter here is the reservoir thickness D. Our estimate above is

TABLE 3. Heat Loss for the Newcastle Geothermal System

	Contour Interval, Wm^{-2}	Area, 10^6 m^2	Average Heat Flow, Wm^{-2}	Heat Loss, MW
	0.5–1.0	3.2	0.75	2.4
	1.0–1.5	2.2	1.25	2.7
	1.5–2.0	1.5	1.75	2.5
	2.0–2.5	1.3	2.25	2.9
	>2.5	1.2	2.75	3.2
Total		9.4		13.7
Background heat loss (0.1 Wm^{-2}) × (9.4 × 10^6 m^2) =				0.9
Anomalous heat loss				12.8

based on the model that most of the thermal anomaly is caused by lateral flow in a thermal aquifer from 75 to 100 m below the surface. An alternative approach would be to try to estimate the value (AD) of a reservoir defined by the upflow region. The appropriate depth D might now be construed to be the interval from 75 m to a depth 2 km, the approximate depth at which the background gradient produces the reservoir temperature, and A to be 1.2×10^6 m, the area enclosed by the highest heat flow contour. Reservoir thermal energy Q_R in this case is 5.9×10^{17} J. Other uncertainties involve reservoir temperature, estimated to be 137°C and 196°C from quartz conductive and Na/K/Ca geothermometers, but again we have taken a conservative value of actual measured temperature, consistent with a minimum estimate procedure. Our estimates of reservoir thermal energy for Newcastle are somewhat less than the value of $1.9 \pm 0.9 \times 10^{18}$ J given by *Brook et al.* [1978] and reflect principally our different view of the reservoir character in this type of geothermal system.

SUMMARY

Twenty-five new regional heat flow values for the Escalante Desert region of southwest Utah confirm a pattern of high but variable heat flow for the Great Basin. The variability is probably caused by deep groundwater flow causing a redistribution of the regional heat flux. The best estimate of a background thermal regime comes from 10 sites in tuffs surrounding the Escalante Desert drilled specifically for heat flow measurements. Here the average geothermal gradient is 56.4°C km^{-1} (s.d. = 12.1) and the mean heat flow is 100 mW m^{-2} (s.d. = 22). Localized heat flow anomalies in the Black Mountains and near Newcastle may indicate promising geothermal prospects.

A blind geothermal system southwest of Newcastle, Utah, has been analyzed, utilizing detailed temperature-depth profiles from 10 drillholes and other geologic and hydrologic information. Heat flow determinations for the 11 wells reveal an area of about 10 km^2 where heat flow is 500 mW m^{-2} or greater. Heat flow maxima exceeding 3 W m^{-2} were measured at two sites. The anomalous thermal power loss at Newcastle is about 13 MW, corresponding to a mass discharge of 32 kg s^{-1} for the system. Conventional estimates of the reservoir thermal energy have also been made; the values are between 6.0×10^{16} J and 5.9×10^{17} J, but it is argued that the 13-MW thermal power loss is a more useful number for the classification of such systems.

We note, finally, that the Newcastle geothermal system has multiple uses; in a practical sense for domestic and agricultural space heating purposes, while in a more esoteric sense for stimulating our ideas on genetic models for Basin and Range geothermal systems.

Acknowledgments. We acknowledge the assistance of John Bodell and Bill Sill who assisted with some of the regional heat flow measurements. Reed Mower provided a compilation of drillhole locations, which was particularly valuable. Eugene Rush kindly gave us permission to use his temperature data at Newcastle, prior to its final release as a U.S. Geological Survey Professional Paper, and has reviewed this paper. Rick Allis made constructive suggestions about the Newcastle system. This work was supported under USGS Geothermal Research Program Grant 14-08-0001-G-544 and DOE/DGE Grant DE-AC07-80ID12079.

REFERENCES

Birch, F., Flow of heat in the Front Range, Colorado, *Geol. Soc. Am. Bull., 61,* 630–657, 1950.

Blackwell, D. D., Heat flow and energy loss in the western United States, in Cenozoic Tectonics and Regional Geophysics of the Western Cordillera, *Mem. Geol. Soc. Am., 152,* 175–208, 1978.

Bodvarsson, G., Temperature inversions in geothermal systems, *Geoexploration, 11,* 141–149, 1973.

Brook, C. A., R. H. Mariner, D. R. Mabey, J. R. Swanson, M. Guffanti, and L. J. P. Muffler, Hydrothermal convection systems with reservoir temperatures ≥90°C, *U. S. Geol. Surv. Circ. 790,* 18–86, 1978.

Chapman, D. S., Heat flow and heat production in Zambia, Ph.D. thesis, Univ. of Mich., Ann Arbor, 1976.

Clement, M. D., Heat flow and geothermal assessment of the Escalante Desert, part of the Oligocene to Miocene volcanic belt in southwestern Utah, M.S. thesis, Univ. of Utah, Salt Lake City, 1980.

Cook, K. L., and E. Hardman, Regional gravity survey of the Hurricane fault area and Iron Springs District, Utah, *Geol. Soc. Am. Bull., 78,* 1063–1076, 1967.

Costain, J. K., and P. M. Wright, Heat flow at Spor Mountain, Jordan Valley, Bingham, and La Sal, Utah, *J. Geophys. Res., 78,* 8687–8698, 1973.

Crosby, G. W., Regional structure in southwestern Utah in geology of the Milford area, *Utah Geol. Assoc. Publ., 3,* 27–32, 1973.

Gardner, S., J. M. Williams, and D. B. Hoover, Audio-magnetotelluric data log and station location map for Lund Known Geothermal Resource Area, Utah, *U. S. Geol. Surv. Open-File Rep., 76-410,* 1976.

Goode, H. D., Thermal waters of Utah, *Utah Geol. Min. Surv. Rep., 129,* 1978.

Hausel, W. D., and W. P. Nash, Petrology of Tertiary and Quaternary volcanic rocks, Washington County, southwestern Utah, *Geol. Soc. Am. Bull., 88,* 1831–1842, 1977.

Hintze, L. F., Geologic map of southwest Utah, Utah Geol. Mineral. Surv., Salt Lake City, Utah, 1963.

Kilty, K., and D. S. Chapman, Convective heat transfer in selected geologic situations, *Groundwater, 18*(4), 386–394, 1980.

Kilty, K., D. S. Chapman, and C. W. Mase, Forced Convective heat transfer in the Monroe Hot Springs geothermal system, *J. Volcanol. Geotherm. Res., 6,* 257–277, 1979.

Lachenbruch, A. H., and J. H. Sass, Models of an extending lithosphere and heat flow in the Basin and Range province, in Cenozoic Tectonics and Regional Geophysics of the Western Cordillera, *Mem. Geol. Soc. Am., 152,* 209–250, 1978.

Lachenbruch, A. H., M. L. Sorey, R. E. Lewis, and J. H. Sass, The near-surface hydrothermal regime of Long Valley Caldera, *J. Geophys. Res., 81*(5), 763–768, 1976.

Mackin, J. H., Some structural features of the intrusions in the Iron Springs District, *Guideb. Geol. Utah, 2,* 1947.

Mackin, J. H., Structural significance of Tertiary volcanic rocks in southwestern Utah, *Am. J. Sci., 258,* 81–131, 1960.

Mase, C. W., D. S. Chapman, and S. H. Ward, Geophysical study of the Monroe-Red Hill geothermal system, *Topical Rep. EY-76-S-07-1601,* 89 pp., Dep. of Geol. and Geophys., Univ. of Utah, Salt Lake City, 1978.

Mase, C. W., S. P. Galanis, Jr., and R. J. Munroe, Near-surface heat flow in Saline Valley, California, *U. S. Geol. Surv. Open-File Rep., 79-1136,* 1979.

Noble, D. C., Some observations on the Cenozoic volcano-tectonic evolution of the Great Basin, western United States, *Earth Planet. Sci. Lett., 17,* 142–150, 1972.

Pe, W., Gravity survey of the Escalante Desert and vicinity in Iron and Washington Counties, Utah, M.S. thesis, Univ. of Utah, Salt Lake City, 1980.

Ratcliffe, E. H., Thermal conductivities of fused and crystalline quartz, *Brit. J. Appl. Phys., 10,* 22–25, 1959.

Rowley, R. D., J. J. Anderson, P. L. Williams, and R. J. Fleck, Age of structural differentiation between the Colorado Plateaus and Basin and Range provinces in southwestern Utah, *Geology, 6,* 51–55, 1978.

Roy, R. F., E. R. Decker, D. D. Blackwell, and F. Birch, Heat flow in the United States, *J. Geophys. Res., 73,* 5207–5221, 1968.

Rush, F. E., Subsurface-temperature data for some wells in southwestern Utah, *U. S. Geol. Surv. Open-File Rep., 77-132,* 1977.

Sass, J. H., and R. J. Munroe, Basic heat-flow data from the United States, *U. S. Geol. Surv. Open-File Rep., 74-9,* 1974.

Sass, J. H., and E. A. Sammel, Heat flow data and their relation to ob-

served geothermal phenomena near Klamath Falls, Oregon, *J. Geophys. Res., 81,* 4863–4868, 1976.

Sass, J. H., A. H. Lachenbruch, and R. J. Munroe, Thermal conductivity of rocks from measurements on fragments and its application to heat flow measurements, *J. Geophys. Res., 76,* 3391–3401, 1971*a*.

Sass, J. H., A. H. Lachenbruch, R. J. Munroe, G. W. Greene, and T. H. Moses, Jr., Heat flow in the western United States, *J. Geophys. Res., 76,* 6376–6413, 1971*b*.

Sass, J. H., S. P. Galanis, Jr., R. J. Munroe and T. C. Urban, Heat flow data from southeastern Oregon, *U. S. Geol. Surv. Open-File Rep., 76-217,* 1976.

Schmoker, J. W., Analysis of gravity and aeromagnetic data, San Francisco Mountains and vicinity, southwestern Utah, *Bull. Utah Geol. Mineral. Surv., 98,* 1972.

Sorey, M. L., R. E. Lewis, and F. H. Olmsted, The hydrothermal system of Long Valley Caldera, California, *U. S. Geol. Surv. Prof. Pap., 1044-A,* 1978.

Stewart, J. H., and J. E. Carlson, Cenozoic rocks of Nevada, *Map 52,* Nev. Bur. of Mines and Geol., Reno, 1976.

Ward, S. H., W. T. Parry, W. P. Nash, W. R. Sill, K. L. Cook, R. B. Smith, D. S. Chapman, F. H. Brown, J. A. Whelan, and J. R. Bowman, A summary of the geology, geochemistry, and geophysics of the Roosevelt Hot Springs Thermal area, Utah, *Geophysics, 43*(7), 1515–1542, 1978.

Wilson, W. R., and D. S. Chapman, Thermal studies at Roosevelt Hot Springs, *Geophysics,* in press, 1981.

Wright, P. M., Geothermal gradient and regional heat flow in Utah, Ph.D. thesis, Dep. of Geol. and Geophys., Univ. of Utah, Salt Lake City, 1966.

(Received November 26, 1980;
revised August 17, 1981;
accepted August 21, 1981.)